JOURNAL OF SPACECRAFT AND ROCKETS
Vol. 38, No. 6, November–December 2001

Spacecraft Charging at Geosynchronous Altitudes: New Evidence of Existence of Critical Temperature

Shu T. Lai*
U.S. Air Force Research Laboratory, Hanscom Air Force Base, Massachusetts 01731-3010
and
Devin J. Della-Rose†
U.S. Air Force Institute of Technology, Wright–Patterson Air Force Base, Ohio 45433-7765

The onset of spacecraft charging in a Maxwellian space environment is independent of the ambient electron density, ion density, and ion temperature but depends solely on a critical, or threshold, electron temperature. Below it, no spacecraft charging occurs; above it, spacecraft charging occurs. The spacecraft-charging potential is determined by the balance of all currents, including the incoming electrons, outgoing electrons, and ambient ions. Abundant evidence from the Los Alamos National Laboratory (LANL) geosynchronous-satellite data supports the existence of critical temperature for the onset of spacecraft charging. Comparison of the theoretical curve with observations on the LANL-1994-084 satellite is encouraging. Whereas the electron-induced secondary-electron coefficient controls the onset of spacecraft charging at about from −1 to −2 kV, the backscattered-electron emission coefficient and the ion-induced electron emission coefficient, which is commonly neglected, control the charging level at higher potentials beyond about from −3 to −4 kV.

Nomenclature

A, B, C	=	parameters in the standard $\eta(E)$ formula
a, b, c	=	parameters in the standard $\delta(E)$ formula
E	=	energy
$E_{\max}$	=	energy at which secondary-electron emission is maximum
e	=	elementary charge
e_e, e_i	=	electron and ion charge, −e, and e, respectively
f	=	distribution function
$I_e(\phi), I_i(\phi)$	=	ambient electron and ion flux, respectively, as functions of spacecraft potential
k	=	Boltzmann's constant
m	=	mass of electron
n	=	electron density
T_e, T_i	=	electron and ion temperatures, respectively
T^*	=	critical, or threshold, temperature
α	=	exponent of the Langmuir orbit-limited current-collection term; geometrical factor for the attracted species in the Mott–Langmuir equation
γ	=	ion-induced secondary-electron emission coefficient
δ	=	secondary-electron emission coefficient
$\delta_{\max}$	=	maximum value of secondary-electron emission
η	=	backscattered-electron emission coefficient
λ	=	reduction factor of the beam current emitted
μ	=	geometrical factor for the repulsed species in the Mott–Langmuir equation
ν	=	reduction factor of the photoelectron current emitted
ϕ	=	spacecraft surface potential

Introduction

IT has been observed,[1,2] though with only a few data points, that the spacecraft potential ϕ measured on the ATS-5 and ATS-6 satellites at geosynchronous altitudes was proportional, with statistical scatter, to the electron temperature T. Linear extrapolation of the data points to $\phi(T) = 0$ showed that the intercept T^* was finite. No explanation of the intercept was available at that time. Subsequent theories[3–6] showed that, indeed, there exists a critical or threshold temperature T^* at which spacecraft charging onsets. Since then, there have been no reports on systematic observation of spacecraft charging as a function of the space plasma electron temperature. Recently, however, with the availability of the Los Alamos National Laboratory (LANL) geosynchronous-satellite (LANL-1989-046, LANL-1990-095, LANL-1991-80, LANL-1994-084, and LANL-97A) data of charging and space environment parameters, we have found that there exists concrete evidence confirming the existence of critical temperature T^* for the onset of spacecraft charging. This paper reports mainly the new evidence for critical temperature. The evidence is not only abundant but is seen almost every time charging onsets. We begin with discussions of physical concepts and simple derivations. The formulations are for uniform surface charging of spacecraft at the geosynchronous environment only. High-level differential charging of spacecraft surfaces and bootstrap charging of isolated small surfaces require special treatments involving many-body interactions between surfaces. Spacecraft charging in low Earth orbits is due to different causes, such as electric fields induced on tethers moving across the ambient magnetic field lines and the depletion of ions in spacecraft wakes. Deep dielectric charging will not be addressed here. The concept of temperature is, strictly speaking, valid for Maxwellian distributions only, because temperature is undefined for nonequilibrium distributions.

Critical, or Threshold, Temperature

At geosynchronous altitudes, the ambient electron flux is about two orders of magnitude larger than that of ions.[7] Figure 1 shows a typical example of the vastly different ion and electron fluxes measured on a LANL geosynchronous satellite. When the onset of spacecraft charging is studied, it is a good approximation to ignore the ions. In this approximation, the incoming electron current is balanced by the outgoing electron current.

To calculate the currents and fluxes, it is convenient to convert the velocity integration to an energy integration because the secondary-electron coefficient $\delta(E)$ and the backscattered-electron coefficient $\eta(E)$ are measured as functions of energy E. At the threshold of spacecraft charging onset, the spacecraft and plasma environment are at the same potential. The current balance equation is given by

Received 14 September 2000; revision received 8 June 2001; accepted for publication 12 June 2001.

*Senior Physicist, Space Vehicles Directorate. Senior Member AIAA.
†Assistant Professor, Department of Engineering Physics. Major, U.S. Air Force.

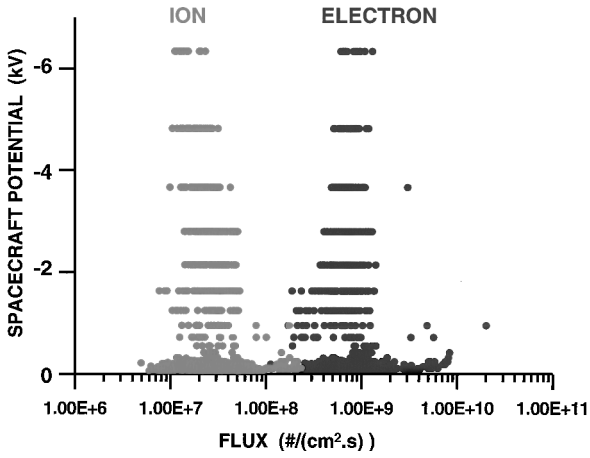

Fig. 1 Spacecraft potential as a function of electron and ion fluxes measured on LANL-1994-084; eclipse periods, March 2000.

$$\int_0^\infty \mathrm{d}EEf(E) = \int_0^\infty \mathrm{d}EE[\delta(E) + \eta(E)]f(E) \qquad (1)$$

where $\delta(E)$ and $\eta(E)$ are independent of the electron density n and electron temperature T of the ambient plasma. Substituting the Maxwellian electron distribution $f(E)$,

$$f(E) = n(m/2\pi kT)^{\frac{1}{2}} \exp(-E/kT) \qquad (2)$$

in Eq. (1), one finds that the density n cancels out on both sides. Equation (1) is independent of the plasma density n. Therefore, in the single Maxwellian model, the plasma density plays no role in the onset of spacecraft charging. Equation (1) is then a function of electron temperature T only. The value of T satisfying Eq. (1) is the critical temperature T^*, at which the incoming electron flux balances the outgoing electron flux.

A simpler way to write Eq. (1) is as follows:

$$\langle \delta + \eta \rangle = 1 \qquad (3)$$

where the notation $\langle\ \rangle$ denotes averaging in the following manner:

$$\langle \delta + \eta \rangle = \frac{\int_0^\infty \mathrm{d}EE[\delta(E) + \eta(E)]f(E)}{\int_0^\infty \mathrm{d}EEf(E)} \qquad (4)$$

A way to help understand the concept of critical temperature is as follows. The factor $[\delta + \eta]$ exceeds unity for a range of low energies, typically 40 and 1600 eV depending on the surface material. That is, the incoming electrons with energies in the low-energy range would be responsible for positive charging, whereas those with higher energies would be responsible for negative charging. These two populations of incoming electrons compete with each other. Because the population of high-energy electrons increases as the temperature increases, negative charging gains favor as the temperature exceeds the critical temperature.

To summarize this section, one has a theorem: There exists a critical or threshold temperature T^* for the onset of spacecraft charging in the Maxwellian model. To demonstrate this theorem mathematically, one needs to use explicit formulas of $\delta(E)$ and $\eta(E)$ as follows.

The Sternglass[8,9] formulas are classics, the Sanders and Inouye[10] $\delta(E)$ formula is convenient, the Prokopenko and Laframboise[11] $\eta(E)$ formula is useful, and a more up-to-date discussion is given by Scholtz et al.[12] The secondary- and backscattered-electron emission properties depend on the surface smoothness, the composition of the material, and the aging of the surface due to UV, reactions with atomic oxygen, and bombardment of electrons and ions in space. Therefore, the surface properties of materials change in space,[13] albeit slowly. For most purposes, it is often sufficient to use approximate formulas.

For analytical calculations of Eq. (1), it is convenient to use the secondary-electron formula of Sanders and Inouye[10]:

$$\delta(E) = c[\exp(-E/a) - \exp(-E/b)] \qquad (5)$$

Table 1 Critical temperatures, eV

Material	Isotropic	Normal
Mg	400	——
Al	600	——
Kapton	800	500
Al oxide	2,000	1,200
Teflon	2,100	1,400
Cu–Be	2,100	1,400
Glass	2,200	1,400
SiO_2	2,600	1,700
Silver	2,700	1,200
Mg oxide	3,600	2,500
Indium oxide	3,600	2,000
Gold	4,900	2,900
Cu–Be (activated)	5,300	3,700
MgF_2	10,900	7,800

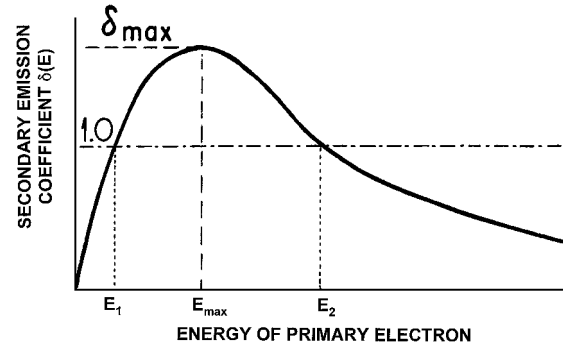

Fig. 2 Secondary electron emission coefficient as a function of primary electron energy.

where $a = 4.3E_{\max}$, $b = 0.367E_{\max}$, and $c = 1.37\delta_{\max}$. The two parameters $E_{\max}$ and $\delta_{\max}$ characterize the energy-dependent behavior of $\delta(E)$ for the surface material (Fig. 2).

The backscattered-electron formula of Prokopenko and Laframboise[11] has the form

$$\eta(E) = A - B\exp(-CE) \qquad (6)$$

where A, B, and C depend on the surface material.

When Eqs. (5) and (6) are used, the current-balance equation becomes[14]

$$c[(1 + kT/a)^{-2} - (1 + kT/b)^{-2}] + A - B(CkT + 1)^{-2} = 0 \qquad (7)$$

which can be solved for given values a, b, c, A, B, and C of the surface material. The solution $T = T^*$ is the critical temperature.

For primary electrons arriving at various angles of incidence θ, one needs to use formulas of $\delta(E, \theta)$ and $\eta(E, \theta)$ and integrate over energy and angles in the current-balance equation. Part of the results[3–6,14] in Table 1 have been cited in Ref. 15 (p. 171); also see Ref. 16.

Spacecraft as a Langmuir Probe

In this paper, spacecraft potential means the equilibrium potential of a spacecraft with respect to the ambient plasma. According to Kirchhoff's law, the sum of currents at every junction in a circuit at equilibrium must be zero. For a typical spacecraft at geosynchronous altitude, it takes a millisecond to reach equilibrium.[2] The equilibrium time depends mostly on the surface capacitance. The equilibrium potential of a spacecraft is given by the current-balance equation. That is, the sum of currents is zero. The equation is the same as that of a langmuir probe.

For the onset of spacecraft charging in the geosynchronous environment, one ignores the ions because the ion current is about two orders of magnitude smaller than that of the electrons. To determine the resulting spacecraft equilibrium (negative) potential, one needs to include the ions that are attracted. If the ion currents are ignored so that the current balance is between the incoming electrons and

the outgoing electrons only, the equilibrium spacecraft potential becomes indeterminate (see the Appendix).

It is often a good approximation to describe the current collection in the geosynchronous space environment by using the orbit-limited Mott–Langmuir equation:

$$\sum I(\phi) = I_i(0)\left(1 - \frac{e_i\phi}{kT_i}\right) - I_e(0)\exp\left(-\frac{e_e\phi}{kT_e}\right) = 0 \qquad (8)$$

where $I_e(\phi)$ and $I_i(\phi)$ are the currents of the repelled and attracted species, respectively, collected by the spacecraft at potential ϕ. Equation (8) is a current-balance equation. In this simple form, Eq. (8), we refer to the current-balance equation as ideal.

Equation (8) can be written as

$$-e_e\phi/kT_e = \log_e[I_i(0)/I_e(0)] + \log_e(1 - e_i\phi/kT_i) \qquad (9)$$

For the approximation of $e\phi/kT_i, \ll 1$, expansion of the log term gives

$$-e_e\phi/kT_e = \log_e[I_i(0)/I_e(0)] - e_i\phi/kT_i - \tfrac{1}{2}(e_i\phi/kT_i)^2 + \cdots \qquad (10)$$

Let $T_i = sT_e$. When $e_e = -e$ and $e_i = e$, where e is the elementary charge, we rearrange Eq. (10) as a quadratic equation:

$$\tfrac{1}{2}(e\phi/kT_i)^2 + (s+1)(e\phi/kT_i) - \log_e[I_i(0)/I_e(0)] + \cdots = 0 \qquad (11)$$

If the first term, $\frac{1}{2}(e\phi/kT_i)^2$ can be neglected in Eq. (11), we have

$$e\phi = [s/(s+1)]kT_e \log_e[I_i(0)/I_e(0)] + \cdots \qquad (12)$$

where the $\log_e$ term value is negative if $I_e(0)$ exceeds $I_i(0)$. Similarly, if $e\phi \ll kT_e$, one obtains a linear dependence of $e\phi$ on kT_e.

The linear dependence of $e\phi$ on kT in Eq. (12) should not be misinterpreted as a straight line because the ratios of ion-to-electron temperatures and ion-to-electron fluxes vary and fluctuate. Figure 3 shows the ion-to-electron temperature ratio as a function of spacecraft potential observed on LANL-1994-084 in September 2000. Figure 4 shows the ion-to-electron flux ratio during the same periods. The ratio has a value of 0.04–0.05 and decreases slightly at higher negative potentials.

Deviations from the Ideal Model

The spacecraft geometry may not be spherical. Other currents may need to be included. These two factors render the model nonideal.

Nonideal Geometry

When Langmuir derived his probe equation, he offered the results in two geometries, namely, a sphere and an infinite cylinder:

$$\sum I(\phi) = \mu I_i(0)\left(1 - \frac{e_i\phi}{kT}\right)^{\alpha} - I_e(0)\exp\left(-\frac{e_e\phi}{kT}\right) \qquad (13)$$

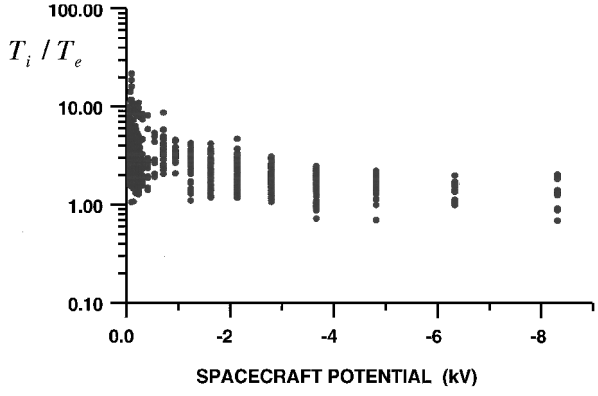

Fig. 3 Ratio of the ion-to-electron temperatures in eclipse, LANL-1994-084, Sept. 2000.

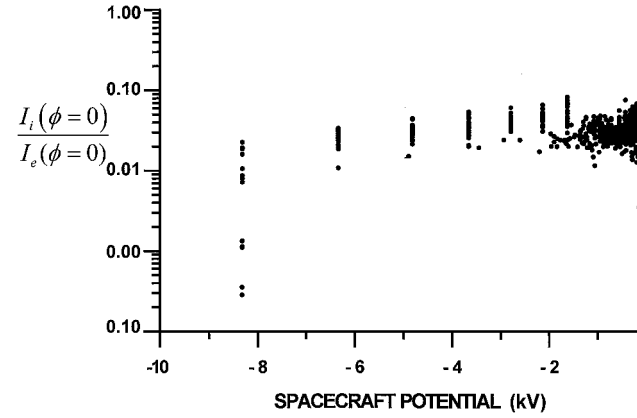

Fig. 4 Ratio of ambient ion flux to ambient electron flux, LANL-1994-084, March, 2000; only points with potential exceeding − 30 V are shown.

where the exponent α is 1 for a spherical probe and $\frac{1}{2}$ for an infinite cylinder and where $\mu = 1$ for a sphere and $\mu = 1.1$ for an infinite cylinder. For arbitrary geometries, there is no guarantee that the probe equation can resemble Eq. (13).

For the SCATHA satellite, which has about the same height as its diameter, Lai[17] analyzed the current-voltage data during varying electron-beam emission from the satellite on quiet days and found $\alpha = 0.774$ for that satellite.

Inclusion of All Currents

When all currents are included, the Mott–Langmuir equation is of the form

$$I_i(0)(1 + \langle\gamma\rangle)(1 - e_i\phi/kT_i)^{\alpha} - I_e(0)(1 - \langle\delta + \eta\rangle) \times \exp(-e_e\phi/kT_e) + \nu I_{\text{ph}} + \lambda I_{\text{beam}} = 0 \qquad (14)$$

where I_{ph} is the photoelectron current, I_{beam} is the current of beams emitted from the spacecraft, $\langle\delta + \eta\rangle$ is defined as in Eq. (4), and γ is the ion-impact-induced secondary-electron emission coefficient:

$$\langle\gamma\rangle = \frac{\int_0^{\infty} \mathrm{d}E\, E f_i(E)\gamma(E - e_i\phi)}{\int_0^{\infty} \mathrm{d}E\, E f_i(E)} \qquad (15)$$

where f_i is the Maxwellian ion distribution of temperature T_i. Because photoelectron and beam emissions are reduced by differential charging, space-charge saturation, and certain beam properties, factors $\nu(\leq 1)$ and $\lambda(\leq 1)$ are introduced in Eq. (14) to account for the reductions. Photoemission and beam emission from spacecraft are beyond the scope of this paper.

Spacecraft Observations

The LANL geosynchronous-satellite data include spacecraft charging levels and electron temperatures. As a precaution, the LANL spacecraft-potential data at levels of about −8 kV and beyond should not be considered reliable.

Figures 5a and 5b shows spacecraft potential as a function of ion temperature and electron density, respectively. Both data were measured on the LANL-1994-084 satellite during the eclipse periods in September 2000. Figures 5a and 5b show a wide spread of data points without a clear trend. If one had to choose only one environment parameter that correlates well with spacecraft potential, neither ion temperature nor electron density would be the best one.

Figure 6 shows data from the LANL-1997A satellite. Electron temperatures and spacecraft potential are shown for the same time. The plots of temperatures and spacecraft potential appear to be mirror images of each other. Note that there exists a critical temperature below which there is no spacecraft charging. Even though a massive hill (up to about 2 keV) in electron temperature (whether parallel or perpendicular) shows up at around 12:00 UT (universal time), there is no charging. Later, when the temperature climbs to 3–5 keV, spacecraft charging occurs.

This database is useful for studying space-weather problems. For example, a solar-coronal mass ejection (CME) arrived at the Earth's

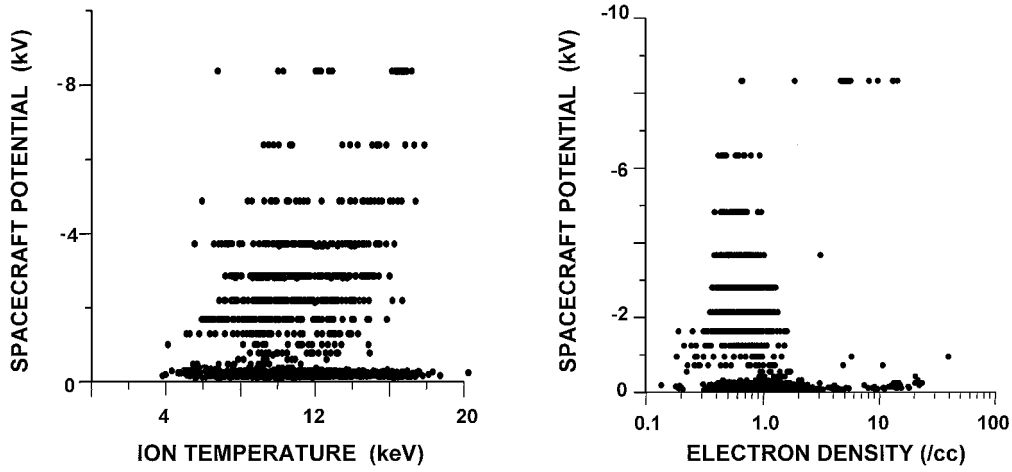

a) Spacecraft potential as a function of ion temperature

b) Spacecraft potential as a function of electron density

Fig. 5 Data from LANL-1994-084 during eclipse periods, Sept. 2000.

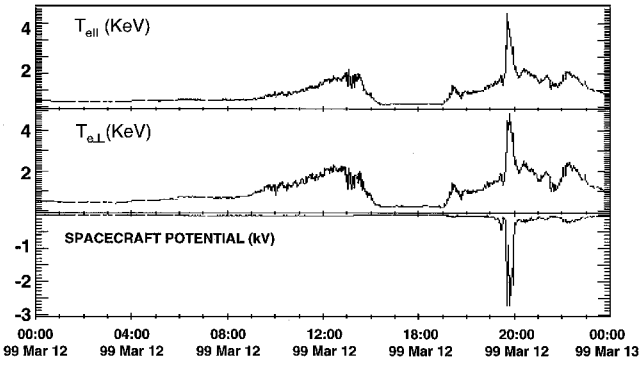

Fig. 6 Mirror behavior of spacecraft potential and electron temperature T_e; note that when T_e is less than a critical value, no charging occurs.

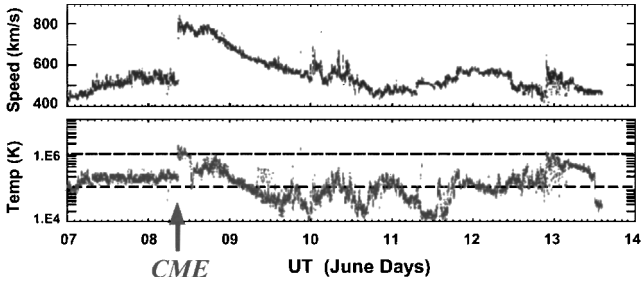

Fig. 7 Arrival of a CME shock, 8 June 2000.

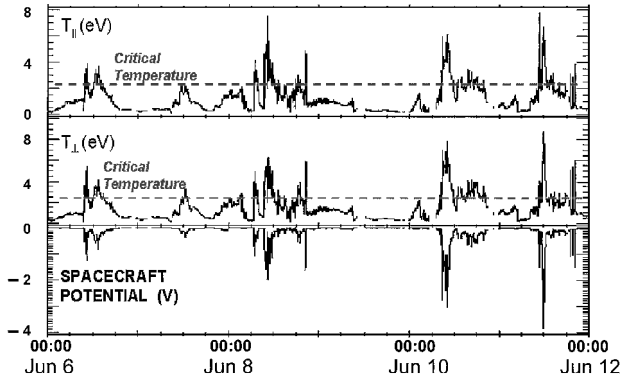

Fig. 8 CME shock front arrived at the ACE satellite, 8:30 UT, 8 June 2000.

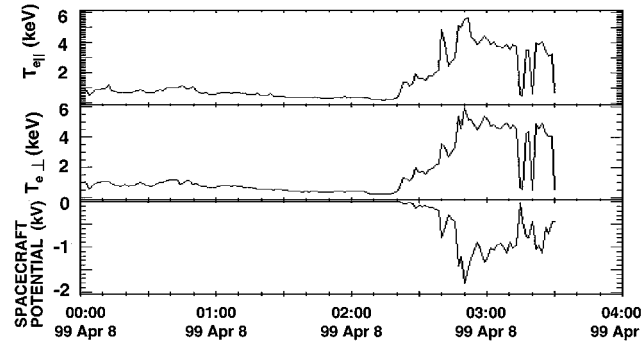

Fig. 9 Mirror behavior of spacecraft potential and electron temperature T_e.

geosynchronousenvironment on 8 June 2000. The Advanced Composition Explorer (ACE) satellite detected the CME shock front arrival at about 8:20 UT (Fig. 7). At the shock front, the wind speed jumped, as did the electron temperature. The temperature rise was due not to the usual mechanism of snapback of the magnetotail but to electron heating at the CME shock front directly. Figure 8 shows that, at about 8:30 UT, the electron temperature at LANL-97A rose sharply, while the spacecraft potential rose at about the same rate as the electron temperature.

This phenomenon of charging dependence on electron temperature also persists, with minor fluctuations, if one examines other satellites or other periods. Figure 9 shows some data taken from the LANL-1990-095 satellite. Again, the phenomenon of a mirror image and a critical temperature is evident.

We present some typical data of a longer period in Fig. 10, which shows the data taken from the LANL-97A satellite from a longer continuous period, from 5 March to 17 March 1999. Again, the gross features of mirror image and the existence of a critical temperature cannot be missed. The critical temperature is at approximately 2.5 keV. The charging peaks show a periodic structure because energetic plasmas come in earthward from the magnetotail and arrive at the geosynchronousorbit at about midnight local time and the energetic electrons drift eastward because of the Earth's magnetic field configuration. As a result, charging often occurs around midnight and in the early morning hours of local time.

Figure 11 shows the LANL-1994-084 data taken during the entire month of March 2000, whereas Fig. 12 shows those taken in September 2000. The spacecraft potentials appear quantized because of instrument resolution. It is interesting that Figs. 11 and 12 are very much alike on average, despite fluctuations of space environmental parameters such as electron and ion fluxes, magnetic fields, etc., in changing space weather. In both Figs. 11 and 12, the data are split into two trends; the one with lower charging levels correspond to spacecraft charging in sunlight, whereas the higher-level trend corresponds to charging in eclipse.

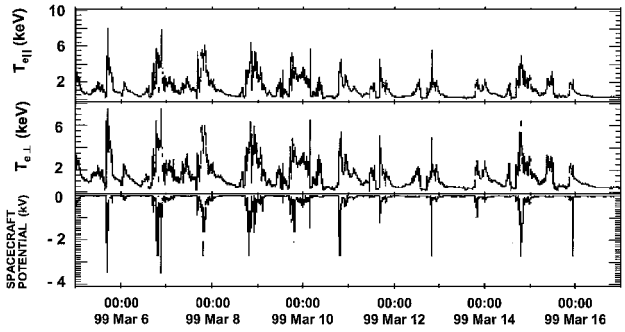

Fig. 10 Mirror behavior of spacecraft potential and electron temperature T_e; note that, when T_e is less than a critical value, no charging occurs.

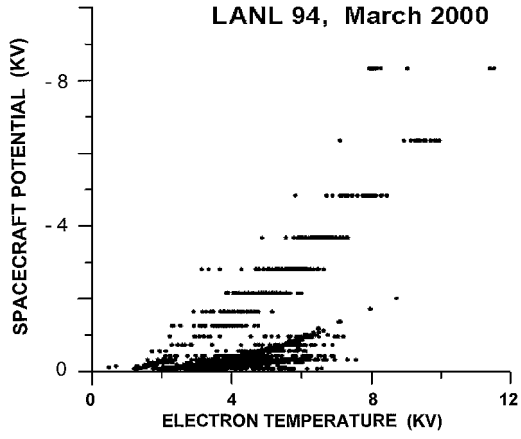

Fig. 11 Potential-temperature curves, LANL-1994-084, March 2000.

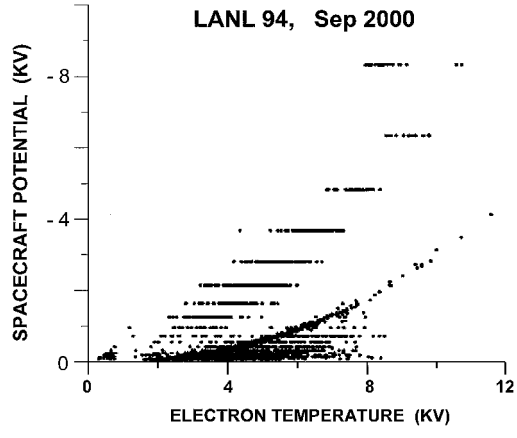

Fig. 12 Potential-temperature curves, LANL-1994-084, Sept. 2000.

It is tempting to superimpose a theoretical curve on the observed data. However, the surface materials on the satellite are unknown, as are the secondary- and backscattered-electron coefficients and the spacecraft geometry. The approximate critical temperature from the data suggests that copper–beryllium (nonactivated), CuBe, is a candidate surface material. The known properties of this alloy are $E_{\max} = 0.3$ keV, $\delta_{\max} = 2.2$, in Eq. (5) and $A = 0.3136$, $B = 0.0692$, and $C = 0.6207$ in Eq. (6). With these properties, the electron-current reduction factor $[1 - \langle \delta + \eta \rangle]$ for various electron temperatures have been calculated (Fig. 13).

The ion-induced secondary-electron emission $\gamma(E)$ coefficient of nonactivated CuBe is unknown. Because aluminum and copper are elements in neighboring groups, we use the $\gamma(E)$ coefficient of aluminum oxide[18]:

$$\gamma(E) = 1.36\left[E^{\frac{1}{2}} \big/ (1 + E/40)\right] \tag{16}$$

The spacecraft potential is then calculated by using the equation for eclipse charging:

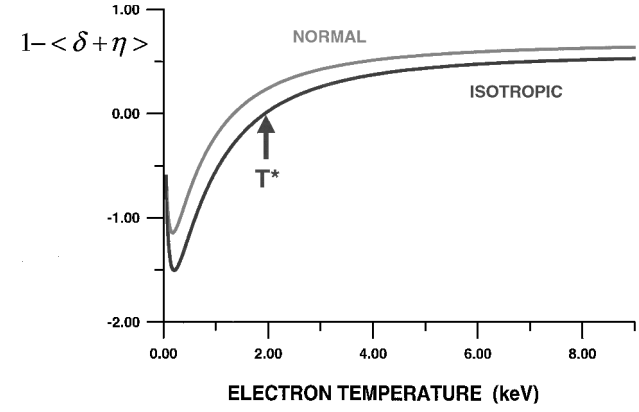

Fig. 13 Reduction factor $1 - \langle \delta + \eta \rangle$ due to secondary and backscattered-electron emissions from copper–beryllium (nonactivated).

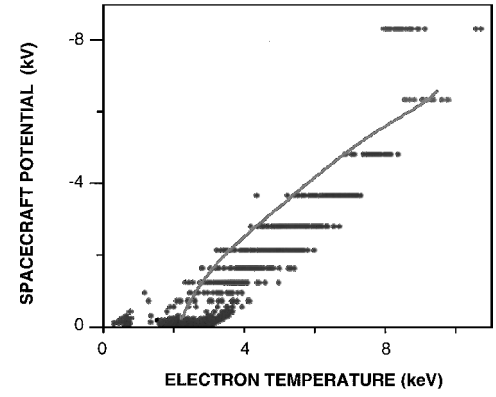

Fig. 14 Comparison of the theoretical curve and the observations during eclipse, LANL-94, Sept. 2000.

$$I_e(0)(1 - \langle \delta + \eta \rangle) \exp[-(e_e\phi/kT_e)]$$
$$= I_i(0)[1 - (e_i\phi/kT_i)](1 + \langle \gamma \rangle) \tag{17}$$

For a simple calculation, we take the ratio of ion-to-electron temperatures as 2 (Fig. 3) and that of ion-to-electron flux as 0.05 (Fig. 4). The calculated spacecraft potential as a function of electron temperature is overlaid on the observed data in Fig. 14. We have tried other materials, but none of these gives a good fit for the entire temperature range. Whereas the secondary-electron emission controls the critical temperature and the charging potential up to a few kilovolts, backscattered-electron and ion-induced secondary-electron emissions, especially the latter, control the high (3 kV and higher) potentials. If, for example, one uses the SCATHA gold paint as the surface material, the high-kilovolt part would fit better, but the critical temperature would not.

Even the critical temperature has uncertainty. We do not know the angle of incidence. Isotropic and normal incidences give slightly different critical temperatures (Fig. 13). As for secondary-electron emission, it is well known that the coefficients can change in time.[13] Ruttenberg and Haas[19] reported that the coefficient $\delta(E)$ for CuBe changes substantially if the alloy is put in an atomic oxygen environment or is at high temperature.

Discussion

The electron temperature is one of the key factors controlling spacecraft charging at geosynchronous altitude. We consider negative charging only because positive charging is often insignificant and requires a very different formulation.

We began by considering a spacecraft initially uncharged. The incoming ambient ion current is naturally much less than that of the ambient electrons. The current balance is between the incoming ambient electrons and the outgoing secondary and backscattered electrons. When a Maxwellian distribution is used, the electron current-balance equation yields a solution, which is the critical,

or threshold, temperature. The existence and the value of the critical temperature depend on the secondary-electron emission and electron-backscattering properties of the surface material. There is no critical electron density. For any other distribution, temperature is undefined.

Once spacecraft charging occurs, ion and electron currents need to be included for spacecraft equilibrium potential determination. The ion collection by a negatively charged spacecraft in the geosynchronous environment is well described by using the Mott–Langmuir equation. For $e\phi \ll kT_e$ or kT_i, the Taylor expansion of this equation yields a linear dependence of spacecraft potential on the ambient plasma temperature. The linear dependence on temperature does not mean a line of constant slope for $\phi(T_e)$ because the ratios of ion-to-electron temperature and ion-to-electron fluxes vary and fluctuate. On average, the approximate linear trend of $\phi(T_e)$ holds. This behavior still holds approximately even if the spacecraft geometry deviates slightly from the sphere. An infinite cylinder or a short cylinder such as SCATHA would also yield similar results.

Given the concept of critical temperature, one can predict the onset of spacecraft charging if one can predict the electron temperature. The magnitude of the critical temperature depends on the surface properties. Table 1 gives the critical temperatures for a number of common spacecraft surface materials.

The LANL satellite data provide abundant evidence of critical temperature. The electron temperatures (parallel or perpendicular) and the spacecraft potential, both plotted vs time, show a mirror image. That is, once the critical temperature is reached, there is a strong correlation between T_e and spacecraft potential; the higher the temperature is, the higher the magnitude of the spacecraft potential (plotted as negative) . This mirror-image phenomenon persists day after day, month after month, and whichever LANL satellite data one chooses. Furthermore, the data show that when the temperature is below a critical value, no charging occurs. This phenomenon is persistent. The value of the critical temperature depends on the surface materials of the satellite.

We have compared the theoretical $\phi(T_e)$ curve with the observations in eclipse on LANL-94. To compare the curve with the observed data for the entire potential range from near 0 V to about -6 kV, one needs to know both the secondary-emission coefficients (for the critical temperature) and the backscattered and ion-induced secondary-electron emission coefficients (for the slope in the high potentials beyond about -3 kV). The critical temperature value from the data seems to suggest that the surface material is nonactivated CuBe. Because the ion-induced secondary-electron emission coefficient of this alloy is unknown, we use that of aluminum oxide. Although the charging onset and the slope in the high-potential range are good, the overall agreement is not perfect. We would expect a better agreement if the surface properties were better known.

Finally, we caution that both properties, namely, the existence of a critical or threshold temperature for spacecraft charging onset and the linear dependence of spacecraft potential on electron temperature, apply only to the main spacecraft surface (also called spacecraft ground). Charging of small pieces of surfaces that are electrically isolated, that is, with no surface conduction, from larger neighboring surfaces require special treatment. Temperature is a well-defined concept for a Maxwellian distribution only.

Conclusions

The spacecraft-charging data of the LANL geosynchronous satellites provide abundant evidence to firmly support the existence of a critical temperature for the onset of spacecraft charging. When the plasma electron temperature is below this critical level (variously, 400–3000 eV or more, depending on the spacecraft surface material) there will be no spacecraft charging. For spacecraft potentials much less than the electron or ion thermal energies, there is an approximate linear trend of potential as a function of electron temperature. The trend does not mean a line of constant slope because the ratios of ion-to-electron temperatures and of ion-to-electron fluxes vary. The data over entire months show that these ratios are about $T_i/T_e \approx 2$ and $I_i/I_e \approx 0.05$ on the average. Comparison of the theoretical curve with the observed data for the entire potential range (up to -8 kV) is encouraging but could be improved if the surface-material properties were better known. We believe that such a comparison for so wide a range of spacecraft potentials has not heretofore been reported.

Appendix: Indeterminate Spacecraft Potential

We will show that the spacecraft potential as calculated by the balance of the incoming Maxwellian electron current and the outgoing secondary plus backscattered-electron currents is indeterminate. The current balance equation is as follows:

$$\int_0^\infty \mathrm{d}E\,E f(E) \exp\left(\frac{-e\phi}{kT_e}\right) = \int_0^\infty \mathrm{d}E\,E f(E)[\delta(E) + \eta(E)] \exp\left(\frac{-e\phi}{kT_e}\right) \tag{A1}$$

The Maxwellian distribution has a special property in that the potential term, $\exp(-e\phi/kT)$, can be factored out and cancels on both sides in Eq. (A1). The result is that the potential ϕ is indeterminate.

The critical, or threshold, temperature T^* is defined as the value of the ambient electron temperature at which the spacecraft potential commences. Below T^*, the potential is zero or slightly positive, and therefore, the ambient ion current can be neglected. Once negative spacecraft charging commences, the value of the spacecraft potential has to be determined by the balance between the electrons and the ions.

Acknowledgments

The Los Alamos magnetospheric plasma analyzer measurements were obtained from the CDAWeb data service at NASA Goddard Space Flight Center. We are grateful to D. McComas and M. F. Thompsen for permission to use the data. We thank W. J. Burke for reading the manuscript with helpful suggestions. We also thank D. Knecht, W. Blumberg, and A. Smith for correcting typographical errors and careless mistakes in the manuscript.

References

[1]Rubin, A., Garrett, H. B., and Wendel, A. H., "Spacecraft Charging on ATS-5," U.S. Air Force Geophysics Lab., Rept. AFGL-TR-80-0168, ADA-090-508, Hanscom AFB, MA, May 1980.

[2]Garrett, H. C., "The Charging of Spacecraft Surfaces," *Review of Geophysics*, Vol. 19, 1981, pp. 577–616.

[3]Lai, S. T., Gussenhoven, M. S., and Cohen, H. A., "Energy Range of Ambient Electrons Responsible for Spacecraft Charging," *EOS*, Vol. 63, No. 18, 1982, p. 421.

[4]Lai, S. T., Gussenhoven, M. S., and Cohen, H. A., "The Concepts of Critical Temperature and Energy Cutoff of Ambient Electrons in High Voltage Charging of Spacecraft," *Proceedings of the 17th ESLAB Synposium*, edited by D. Guyenne and J. H. A. Pedersen, ESA, Noordwijk, The Netherlands, 1983, pp. 169–175.

[5]Laframboise, J. G., Godard, R., and Kamitsuma, M., "Multiple Floating Potentials, Threshold Temperature Effects, and Barrier Effects in High Voltage Charging of Exposed Surfaces on Spacecraft," *Proceedings of International Symposium on Spacecraft Materials in Space Environment*, ESA SP-178, ESA, Paris, 1982, pp. 269–275.

[6]Laframboise, J. G., and Kamitsuma, M., "The Threshold Temperature Effect in High Voltage Spacecraft Charging," *Proceedings of Air Force Geophysics Workshop on Natural Charging of Large Space Structures in Near Earth Polar Orbit*, U.S. Air Force Research Lab., Rept. AFRL-TR-83-0046, ADA-134-894, Hanscom AFB, MA, 1983, pp. 293–308.

[7]Reagan, J. B., Meyerott, R. E., Nightingale, R. W., Filbert, P. C., and Imhoff, W. L., "Spacecraft Charging Currents and Their Effects on Space Systems," *IEEE Transactions on Electrical Insulation*, Vol. 18, No. 2, 1983, pp. 354–365.

[8]Sternglass, E. J., "Theory of Secondary Electron Emission," Westinghouse Research Lab., Paper 1772, Pittsburgh, PA, 1954.

[9]Sternglass, E. J., "Backscattering of Kilovolt Electrons from Solids," *Physical Review*, Vol. 95, No. 2, 1954, p. 345.

[10]Sanders, N. L., and Inouye, G. T., "Secondary Emission Effects on Spacecraft Charging: Energy Distribution Consideration," *Spacecraft Charging Technology 1978*, edited by R. C. Finke and C. P. Pike, NASA-2071, ADA-084626, U.S. Air Force Geophysics Lab., Hanscom AFB, MA, 1978, pp. 747–755.

[11]Prokopenko, S. M., and Laframboise, J. G. L., "High Voltage Differential Charging of Geostationary Spacecraft," *Journal of Geophysical Research*, Vol. 85, No. A8, 1980, pp. 4125–4131.

[12]Scholtz, J. J., Dijkkamp, D., and Schmitz, R. W. A., "Secondary Electron Emission Properties," *Philips Journal of Research*, Vol. 50, No. 3–4, 1996, pp. 375–389.

[13]Mizera, P. F., and Leung, M. S., "Changes in Electrical Properties of Spacecraft Materials," The Aerospace Corp., Rept. No. SSL-81 (6505-02)-07, El Segundo, CA, May 1981.

[14]Lai, S. T., "Spacecraft Charging Thresholds in Single and Double Maxwellian Space Environments," *IEEE Transactions on Nuclear Science*, Vol. 19, No. 6, 1991, pp. 1629–1634.

[15]Hastings, D., and Garrett, H. B., *Spacecraft-Environment Interactions*, Cambridge Univ. Press, Cambridge, England, U.K., 1997, p. 171.

[16]Olsen, R. C., "A Threshold Effect for Spacecraft Charging," *Journal of Geophysical Research*, Vol. 88, No. A1, 1983, pp. 493–499.

[17]Lai, S. T., "An Improved Langmuir Probe Formula for Modeling Satellite Interactions with Near Geostationary Environment," *Journal of Geophysical Research*, Vol. 99, No. A1, 1994, pp. 459–468.

[18]Whipple, E. C., "Potentials of Surfaces in Space" *Reports on Progress in Physics*, Vol. 44, 1981, pp. 1197–1212.

[19]Ruttenberg, F. E., and Haas, T. W., "Composition and Morphology vs Secondary Electron Yield of Be–Cu Dynodes," *Journal of Vacuum Science and Technology*, Vol. 12, No. 5, 1975, pp. 1043–1046.

A. C. Tribble
Associate Editor